Astronomy & Astrophysics manuscript no. COH2˙complex
July 12, 2016
© ESO 2016

The CO-H_2 van der Waals complex and complex organic molecules in cold molecular clouds: a TMC-1C survey⋆

A. Potapov[1,2], Á. Sánchez-Monge[1], P. Schilke[1], U. U. Graf[1], Th. Möller[1], and S. Schlemmer[1]

[1] I. Physikalisches Institut, Universität zu Köln, Zülpicher Str. 77, 50937 Cologne, Germany
[2] Laboratory Astrophysics Group of the Max Planck Institute for Astronomy at the Friedrich Schiller University Jena, Institute of Solid State Physics, Helmholtzweg 3, 07743 Jena, Germany
e-mail: alexey.potapov@uni-jena.de

Received ; accepted

arXiv:1607.02749v1 [astro-ph.GA] 10 Jul 2016

ABSTRACT

Context. Almost 200 different species have been detected in the interstellar medium (ISM) during the last decades, revealing not only simple species but complex molecules with more than 6 atoms. Other exotic compounds, like the weakly-bound dimer $(H_2)_2$, have also been detected in astronomical sources like Jupiter.
Aims. We aim at detecting for the first time the CO-H_2 van der Waals complex in the ISM, which if detected can be a sensitive indicator for low temperatures.
Methods. We use the IRAM 30m telescope, located in Pico Veleta (Spain), to search for the CO-H_2 complex in a cold, dense core in TMC-1C (with a temperature of $\sim$ 10 K). All the brightest CO-H_2 transitions in the 3 mm (80-110 GHz) band have been observed with a spectral resolution of 0.5–0.7 km s^{-1}, reaching a rms noise level of $\sim$ 2 mK. The simultaneous observation of a broad frequency band, 16 GHz, has allowed us to conduct a serendipitous spectral line survey.
Results. No lines belonging to the CO-H_2 complex have been detected. We have set up a new, more stringent upper limit for its abundance to be [CO-H_2]/[CO] $\sim 5 \times 10^{-6}$, while we expect the abundance of the complex to be in the range $\sim 10^{-8}$–10^{-3}. The spectral line survey has allowed us to detect 75 lines associated with 41 different species (including isotopologues). We detect a number of complex organic species, e.g. methyl cyanide (CH_3CN), methanol (CH_3OH), propyne (CH_3CCH) and ketene (CH_2CO), associated with cold gas (excitation temperatures $\sim$ 7 K), confirming the presence of these complex species not only in warm objects but also in cold regimes.

Key words. astrochemistry – molecular processes – methods: observational – ISM: molecules

1. Introduction

During the last decades, the number of atomic and molecular species detected in the interstellar medium (ISM) has increased considerably thanks to (i) the improved sensitivity of facilities like the IRAM 30m telescope in Spain or the Atacama Large Millimeter/submillimeter array (ALMA) in Chile, and (ii) new laboratory measurements of transitions of new species included in catalogues such as the Cologne Database for Molecular Spectroscopy (CDMS). Almost 200 different species have been found in Galactic/extragalactic environments such as cold dense cores, hot molecular cores, circumstellar disks, evolved stars or large diffuse molecular clouds. These 200 species do not consist only of simple molecules like the most abundant H_2 and CO, but also include complex species usually defined as molecules with 6 or more atoms (Herbst & van Dishoeck 2009; see the CDMS database[1] for a summary of detected species in space).

Molecular hydrogen, H_2, is by far the most abundant molecule in the Universe, followed by carbon monoxide, CO. Therefore, the intermolecular forces between these two species are of fundamental interest. If the CO-H_2 van der Waals complex[2] exists in measurable amounts in the ISM, it could be a sensitive indicator for low temperatures. The binding energy of the complex is so small — typically 20 cm^{-1} or 30 K — that the relative abundance of the complex in the gas phase is expected to increase at lower temperatures.

There is an open debate about the feasibility of observing such weakly-bound species because their formation rates at the very low densities of interstellar molecular clouds (below 10^7 cm^{-3}) are low, due to the small probability of three-body collisions, which is the main formation route of van der Waals complexes in the laboratory. On the other hand, the large timescale on which these processes occur in interstellar space makes radiative association, which is usually a slow process, quite feasible (e.g. Klemperer & Vaida 2006). Also non-equilibrium conditions in the ISM may strongly favor the formation and concentration of the CO-H_2 complex over time on the surfaces of dust grains in shielded regions at low temperatures, with release to the gas-phase occurring by localized heating processes such as turbulence or jets/outflows (e.g. Allen et al. 1997). However, one also has to consider that CO tends to be frozen out onto dust grains in very cold, dense regions, and it seems difficult to release the CO-H_2 complex from grains without destroying it. On the other hand, this is completely unchartered territory, and even sensitive upper limits are useful. A detection of this com-

⋆ Based on observations carried out with the IRAM 30m Telescope. IRAM is supported by INSU/CNRS (France), MPG (Germany) and IGN (Spain).

[1] http://www.astro.uni-koeln.de/cdms/molecules

[2] We note that this complex does not correspond to the formaldehyde molecule, H_2CO.

Table 1: Frequencies of the brightest CO-H_2 targeted lines

	Transition	Frequency (MHz)
CO-paraH_2	(1,1,0)–(0,0,0)	108480.857
	(1,1,1)–(1,0,1)	91012.364
CO-orthoH_2	(2,f,2)–(1,f,1)	101907.919
	(3,e,2)–(2,e,1)	93433.726
CO-orthoD_2	(1,1,0)–(0,0,0)	102791.612
	(1,1,1)–(1,0,1)	89483.510
CO-HD	(1,1,0)–(0,0,0)	105636.

Notes. The uncertainty in the frequency measurements is about 50 kHz for all the transitions, except for CO-HD with a few tens of MHz. The labelling of the quantum numbers of the transitions are explained in detail in Fig. 1.

plex would challenge many beliefs we have about the chemistry of dense molecular clouds.

There have been several attempts to observe complexes containing CO and H_2 molecules. The detection of the H_2 dimer, $(H_2)_2$, in the atmosphere of Jupiter has been reported by McKellar (1988), while searches for the CO dimer, $(CO)_2$ (Vanden Bout et al. 1979), and the CO-paraH_2 complex (Allen et al. 1997) in Galactic molecular clouds were not successful thus far. Laboratory data have clarified later a spectroscopic problem of these unsuccessful searches. The extensive millimeter-wave (MMW) studies of the CO dimer (Surin et al. 2007) have shown that the radio astronomical search of this complex was based on frequencies which cannot be unambiguously attributed to $(CO)_2$. In the case of the CO-paraH_2 complex, the interstellar search was outside the correct frequency position of the most promising R(0) line, as later identified by the first MMW study of CO-paraH_2 (Pak et al. 1999), and only the weaker Q(1) line was correctly tuned.

Recent laboratory studies of the CO-H_2 complex have provided precise MMW frequencies with uncertainties of about 50 kHz for the complex in different spin modifications and for its deuterated isotopologues: CO-paraH_2 (Potapov et al. 2009b), CO-orthoH_2 (Jankowski et al. 2013), CO-orthoD_2 (Potapov et al. 2009a) and CO-HD (Potapov et al. 2015). Therefore, the availability of precise rest frequencies and modern astronomical receivers (with a sensitivity several times better than the old receivers used 20 years ago), combine in a great opportunity to detect for the first time a van der Waals complex in the ISM.

In this paper we present IRAM 30m observations of a cold region in the Taurus molecular cloud in the search for the CO-H_2 van der Waals complex. In Sect. 2 we describe the observations. In Sect. 3 we present the main results. Unfortunately, we do not have a detection of the CO-H_2 complex but we can set a new limit that can be used in future chemical modelling. In addition to the search for the CO-H_2 complex, the IRAM 30m observations allowed us to conduct a spectral line survey of a very cold region ($\sim$ 10 K), and we report the detection of complex organic molecules (COMs) as well as first time tentative detections of species in this object. In Sect. 4 we discuss our results, and we end the paper with a summary of the main results in Sect. 5.

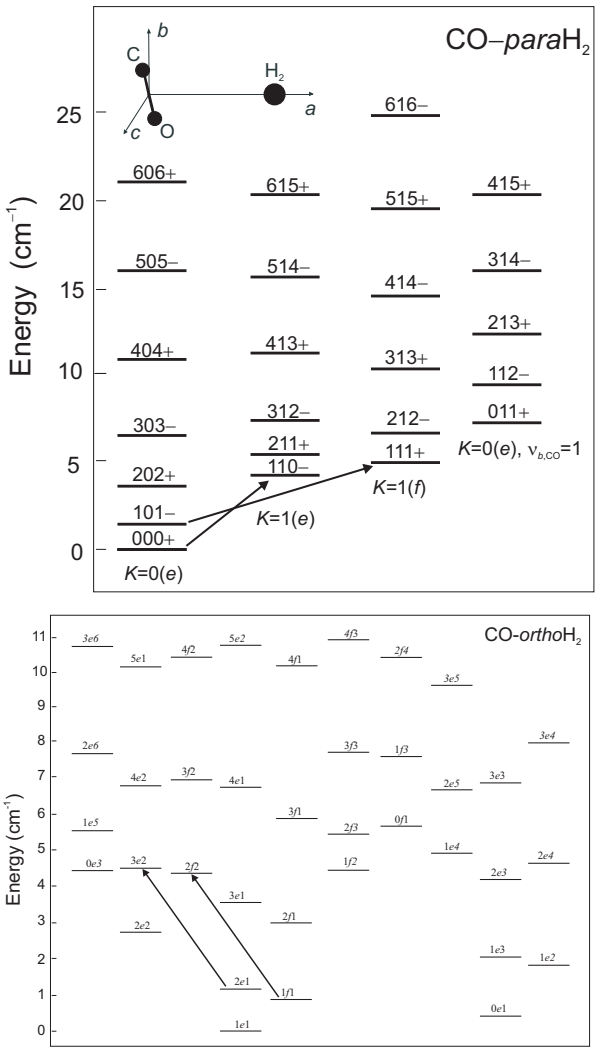

Fig. 1: Energy level diagram for the CO-paraH_2 (top panel) and CO-orthoH_2 (bottom panel) van der Waals complex. *Top panel*: The energy levels are labeled by quantum numbers J, j_{CO} and l where J is the total angular momentum, j_{CO} refers to the rotation of the CO sub-unit and l refers to the end-over-end rotation of the complex. K corresponds to the projection of J onto the intermolecular axis. The labels e and f indicate the parity of the J levels within a given stack. The parity of an even-J level is '+' for stacks labeled by e and '−' for f, while the parity of an odd-J level is '−' for e and '+' for stacks labeled f. The insert shows the approximate geometrical structure of the CO-H_2 complex (see Potapov et al. 2009b for details). *Bottom panel*: The energy levels are labeled by quantum numbers J, parity P and n_J,P, a consecutive number of the state for the given values of J and P (see Jankowski et al. 2013 for details). In both panels, the targeted transitions are indicated by arrows.

2. Observations

The observations were carried out from 2015 May 6 until May 9 at the IRAM 30m telescope, located in Pico Veleta (Granada, Spain) under the project code 131-14. We have chosen to attempt the detection of the CO-H_2 complex in the nearest star forming region: the Taurus molecular cloud complex (e.g. Olano et al. 1988; Suzuki et al. 1992; Roberts & Millar 2000), in particular towards a cold, dense condensation nearby TMC-1C which has measured low excitation temperatures of 3–7 K (Spezzano et al. 2013), and for which a kinetic temperature of 10 K reproduce the observations presented by Spezzano et al. (2016). This object harbours the physical conditions (low temperature and high density, $\sim 4 \times 10^4$ cm^{-3}; Schnee et al. 2007) necessary to search for the CO-H_2 complex. We note that the density is still low enough

to not have all the CO frozen out onto the dust grains[3]. The coordinates used for the observations are $\alpha_{2000} = 04^h41^m16.^s1$ and $\delta_{2000} = +25°49'43.''8$, coincident with the coordinates used in Spezzano et al. (2013).

We tuned the telescope to cover a number of transitions of the CO-H_2 complex and its deuterated isotopologues in the 3 mm band (E090) of the EMIR receiver. All four EMIR sub-bands were connected to the Fast Fourier Transform Spectrometers (FTS), with a spectral resolution of 200 kHz, which results in $\sim$ 0.5–0.7 km s^{-1} at the corresponding frequencies. In Table 1, we list the most intense transitions of the complex covered in our spectral setup. The frequency coverage was selected in order to optimize the simultaneous search of the strongest CO-paraH_2 and CO-orthoH_2 lines. The energy level diagrams for CO-paraH_2 and CO-orthoH_2 are shown in Fig. 1. In total, our observations cover an effective bandwidth of 16 GHz, ranging from 85.87 to 93.65 GHz in the lower sideband, and from 101.55 to 109.33 GHz in the upper sideband. The total observing time was 20 hours. We used the ON-OFF observation mode, with the reference position located at the offset (800″, 600″). The telescope pointing was checked every 1.5 hours and was found to be accurate to $\sim$ 5″, i.e. only a fraction of the beam size of the telescope at these frequencies: $\sim$ 30″. The weather conditions were stable during the observations with zenith opacities of 0.02–0.07 and system temperatures of 80–100 K. The observed spectra was calibrated following the standard procedures, and analyzed using the GILDAS[4] software package. We converted the spectra to the main beam temperature scale, using a forward efficiency of 0.95, and a beam efficiency of 0.79 and 0.81 for the upper and the lower sidebands, respectively. The final spectrum has a noise level of $\sim$ 2 mK.

3. Results and analysis

3.1. The CO-H_2 complex

In Fig. 2 we show, in the top panels, the full spectrum obtained with the IRAM 30m telescope. A number of bright lines have been detected throughout the covered frequency range and they will be discussed in Sect. 3.2. The bottom panels of Fig. 2 show a close-up view of the frequency ranges around the frequencies of the brightest CO-H_2 lines, corresponding to the CO-orthoH_2 and CO-paraH_2 transitions listed in Table 1. No lines belonging to the CO-H_2 complex are detected at the corresponding frequencies (indicated in the figure with red dotted vertical lines). It is important to note that the noise at the high-frequency transitions is slightly larger than the average one (i.e. 2 mK). This larger noise is due to ripples in the baseline that were not possible to completely remove. However, since their wavelength is much larger than the expected linewidths, $\sim$ 0.3 km s^{-1}, they do not affect the search for the CO-H_2 transitions. None of the four transitions have been detected, and we therefore, set an upper limit of $\sim$ 6 mK (corresponding to 3σ) for the intensities of these lines.

[3] Referring to the work of Caselli et al. (1999), a model in which CO is condensed out onto dust grains at densities above 10^5 cm^{-3} and has a roughly canonical abundance at lower hydrogen densities, is supported by the observations of gas-phase depletion in the L1544 cloud core.

[4] The GILDAS software package is developed by the IRAM and Observatoire de Grenoble, and can be downloaded at http://www.iram.fr/IRAMFR/GILDAS

Table 2: Species, temperatures, column densities and transitions detected above 5σ towards TMC-1C (see Sect. 3.2 for details)

Species	T (K)	log(N) (log[cm^{-2}])	Transitions
$^{13}C^{18}O$	7.0	13.30 ± 0.50	1
^{13}CS	7.0	11.65 ± 0.26	1
SO	6.2 ± 0.7	13.25 ± 0.28	2
$S^{18}O$	6.2	11.81 ± 0.26	1
CCH	7.0	13.42 ± 0.11	6
CCS	4.7 ± 0.7	12.95 ± 0.38	4
HCN	7.0	12.26 ± 0.18	1
$H^{13}CN$	7.0	11.51 ± 0.29	1
$HC^{15}N$	7.0	10.71 ± 0.21	1
HNC	7.0	12.92 ± 1.01	1
$HN^{13}C$	7.0	11.76 ± 0.13	1
$H^{15}NC$	7.0	11.51 ± 0.30	1
HCO	6.1 ± 1.8	11.03 ± 0.30	4
HCO^+	7.0	12.09 ± 0.35	1
$H^{13}CO^+$	7.0	11.59 ± 0.38	1
$HC^{17}O^+$	7.0	9.97 ± 1.50	1
DCS^+	7.0	10.88 ± 0.24	1
SO_2	7.0	11.95 ± 0.23	1
N_2H^+	7.0	12.42 ± 0.19	1
CCCS	6.2 ± 0.5	12.67 ± 0.31	2
CCCO	7.0	11.26 ± 0.23	1
c-CCCH	6.0 ± 1.9	12.14 ± 0.35	6
H_2CS	14.8 ± 2.1	12.67 ± 0.15	2
HDCS	14.8	12.01 ± 0.98	1
$H_2C^{34}S$	14.8	11.43 ± 1.59	1
$HOCO^+$	7.0	11.25 ± 0.19	1
HNCO	7.0	13.11 ± 0.11	1
NH_2D	7.0	12.59 ± 1.00	1
C_4H	7.8 ± 0.9	13.12 ± 0.26	2
l-C_3H_2	7.2 ± 0.7	11.18 ± 0.31	3
c-C_3HD	6.0 ± 1.8	12.14 ± 0.35	4
c-C_3D_2	6.0	10.99 ± 1.90	1
CH_2CO	7.0	12.42 ± 0.37	1
HC_3N	4.2 ± 0.3	14.62 ± 0.45	2
HCCNC	7.0	11.81 ± 0.15	1
HCOOH	7.0	11.64 ± 0.13	1
CH_3CN	7.1 ± 1.0	11.80 ± 0.45	2
CH_3OH	7.0	12.86 ± 1.27	1
CH_2DOH	7.0	11.60 ± 0.50	1
CH_3CCH	15.0 ± 3.6	13.31 ± 0.13	3
CH_3CCD	15.0	11.97 ± 0.16	2

3.2. Spectral line survey

The broad frequency range covered with the IRAM 30m telescope permits not only to study the CO-H_2 lines, but also to perform a spectral line survey of this cold dense condensation. It is worth mentioning that the high sensitivity achieved with our observations is adequate to search, e.g., for COMs (molecules with 6 or more atoms) in low-temperature environments. COMs have long been detected in the interstellar medium, especially in hot molecular cores associated with high-mass star forming regions (e.g. Cummins et al. 1986; Blake et al. 1987; Sánchez-Monge et al. 2013, 2014). The advent of sensitive instruments has also revealed a chemical complexity associated with low-mass hot cores (or hot corinos; e.g. Cazaux et al. 2003) and intermediate-mass hot cores (e.g. Sánchez-Monge et al. 2010). Despite their formation routes remain uncertain, both warm gas-phase and grain-surface reactions have been invoked to account for their presence in low-mass protostars. In this latter scheme, COMs result from radical-radical reactions on the grains as radicals become mobile when the nascent protostar warms up its surroundings and the resulting molecules are subsequently desorbed into

the gas phase at higher temperatures or by shock events produced by winds/jets (e.g. Garrod & Herbst 2006). In the last years, the detection of COMs in cold environments (T < 30 K; Bacmann et al. 2012; Vastel et al. 2014) represents a challenge for the chemical models and an opportunity to improve and clarify the role of the grain-surface and gas-phase chemistry.

The top panels of Fig. 2 show the spectral line survey towards the condesantion in TMC-1C. We have identified 75 lines with an intensity > 5σ. We note that the spectral resolution of only 0.5–0.7 km s^{-1} is not enough to resolve most of the lines, suggesting that all they are excited in an environment with a temperature < 30 K, i.e in cold gas[5]. The identification of the lines was done using the CDMS (Müller et al. 2005) and JPL (Pickett et al. 1998) databases, and later on confirmed by creating synthetic spectra of each species using the XCLASS[6] software (Möller et al. 2015). XCLASS is a toolbox for the Common Astronomy Software Applications (CASA) package containing new functions for modeling interferometric and single-dish data. The included myXCLASS program calculates synthetic spectra by solving the radiative transfer equation for an isothermal object in one dimension where the required molecular data are taken from an embedded database containing entries from the CDMS and JPL databases using the Virtual Atomic and Molecular Data Center (VAMDC) portal. The contribution of a molecule is defined by an user-defined number of components where each component is described by four main parameters: excitation temperature, column density, velocity width and velocity offset. In order to achieve a good description of the data we fit these parameters using the included model optimizer package MAGIX (Möller et al. 2013). By performing an internal resampling, XCLASS makes sure that the line is sampled properly, even if the velocity resolution of the data is coarse.

In Table 2 we list the identified species with the corresponding excitation temperature (column 2), column density (column 3) and number of transitions above 5σ (column 4). The 75 detected lines come from 41 different species (including isotopologues) and four unidentified lines at the frequencies 90.593 GHz, 90.602 GHz, 92.872 GHz and 101.981 GHz with main beam temperatures of 18 mK, 18 mK, 30 mK and 15 mK, respectively. For those species with more than one transition we have fitted with XCLASS simultaneously the excitation temperature and column density[7]. If only one transition is detected above 5σ for a given species, we fit only the column density and fix the excitation temperature to 7 K, which corresponds to the average temperature of the other transitions and is consistent with the value measured also in Spezzano et al. (2013). For the different detected isotopologues, we have fixed the excitation temperature to be the same of the main species, and we have fitted only the column density. In all cases we consider a linewidth of 0.3 km s^{-1}. In Fig. 3 we present the whole spectral survey, indicating the location of the different detected transitions. A number of COMs have been detected in this cold dense core. We discuss the results in Sect. 4.2.

[5] Most of the lines are detected in one single channel. The exceptions are species such as HCN and N_2H^+ due to the hyperfine structure, and $^{13}C^{18}O$ with a weak blue-shifted wing. The thermal linewidth for gas at 30 K is 0.23 km s^{-1}, 0.18 km s^{-1} and 0.16 km s^{-1}, for species with mean molecular weights of 25 (e.g. CCH), 40 (e.g. CH_3CCH) and 56 (e.g. CCS), respectively.

[6] The eXtended CASA Line Astronomy Software Suite (XCLASS) can be downloaded at https://www.astro.uni-koeln.de/projects/schilke/XCLASSInterface

[7] For species like C_3H_2 or CH_3OH, with different spin symmetries: ortho/para, the total column density is given.

4. Discussion

4.1. Detectability of the CO-H_2 complex

In Sect. 3.1 we report an upper limit of ∼ 6 mK for the CO-H_2 lines. We follow the same approach as in Allen et al. (1997) to establish an upper limit for the column density of the CO-paraH_2 complex. We use the dipole moment of CO and the total partition function of CO-paraH_2 calculated from the now known energy level scheme of the complex (see Fig. 1). Our calculations result in a value of $\sim 3\times10^{12}$ cm^{-2} for the column density of the complex and a fractional abundance of the CO-paraH_2 dimer relative to CO of $\sim 5\times10^{-6}$, assuming the CO column density to be 6×10^{17} cm^{-2} (derived from the $^{13}C^{18}O$ column density listed in Table 2, and assuming standard $^{12}C/^{13}C$ and $^{16}O/^{18}O$ ratios of 60 and 500, respectively.

In the following, we estimate what number density of the CO-H_2 molecular complex do we expect under the ISM conditions, and compare it to the new upper limit. All the reaction rates used in the following are generic rates, which have not specifically been measured or calculated, and are taken from the review paper by van Dishoeck (2014). The given reactions are the basic types of reactions in space. Following van Dishoeck (2014), there are two basic processes by which molecular bonds can be formed in the interstellar molecular clouds: radiative association and formation on grain surface with subsequent release to the gas phase. In the radiative association process, the binding energy of a new molecule or molecular complex is carried out through the emission of a photon, and can be described as:

$$H_2 + CO \rightarrow CO{-}H_2 + h\nu \quad (1)$$

and proceeds at the rate of a radiative association reaction $k_1 \approx 10^{-17}$–10^{-14} cm^3 s^{-1}. For the case of the formation on grain surfaces, a dust particle accommodates the released energy, and the process can be described as

$$H_2 + CO{-}grain \rightarrow CO{-}H_2 + grain \quad (2)$$

which proceeds at a rate of $k_2 \approx 10^{-17}$ cm^3 s^{-1}.

On the other side, there are three processes for the destruction of the complex: photodissociation, collisional dissociation and neutral-neutral bond rearrangement. The first one can be described by

$$CO{-}H_2 + h\nu \rightarrow products \quad (3)$$

with a reaction rate of $k_3 \approx 10^{-10}$–10^{-8} cm^3 s^{-1}. The second and third ones can be given by

$$CO{-}H_2 + M \rightarrow products \quad (4)$$

where M being a reaction partner, with rates for collisional dissociation of $k_4 \approx 10^{-26}$ cm^3 s^{-1} and for bond rearrangement of $k_5 \approx 10^{-11}$–10^{-9} cm^3 s^{-1}.

We consider a dense condensation with an H_2 density of $[H_2] = 4\times10^4$ cm^{-3}, the CO density given by [CO] = [CO-grain] = 10^{-4} [H_2], and assume [M] = [H_2]. Under these conditions, the formation is dominated by radiative association, while the destruction mainly occurs by the bond rearrangement. As it is stated by van Dishoeck (2014), collisional dissociation of molecules is only important in regions of very high temperature (> 3000 K) and density. Thus, we determine the CO-H_2 abundance in the equilibrium as [CO-H_2] = $(k_1[H_2][CO])/(k_5[M])$ = 4×10^{-8}–4×10^{-3} cm^{-3} and [CO-H_2]/[CO] ∼ 10^{-8}–10^{-3}. The obtained range for a possible abundance of CO-H_2 is quite wide. From the comparison of our estimated [CO-H_2]/[CO] abundance to the upper detection limit of [CO-H_2]/[CO]∼ 5×10^{-6}, we can conclude that the complex might be detected by observations with one or two orders higher sensitivity.

4.2. Molecular inventory in cold regions

Table 2 and Figure 3 reveal a relatively rich chemistry in the cold dense core TMC-1C. Despite the average excitation temperature being of only 7 K, we are able to detect a number of species with 6 or more atoms: CH_3CN, CH_3OH and CH_3CCH. The column densities for these species are in the range 10^{11}–10^{13} cm^{-2}, which results in abundances of 10^{-12}–10^{-10} assuming a H_2 column density of 10^{22} cm^{-2} (e.g. Schnee & Goodman 2005). These abundances are about two orders of magnitude lower than the typical abundances found toward more massive hot molecular cores. We have searched for more complex species, such as methyl formate (CH_3OCHO) or dimethyl ether (CH_3OCH_3), but we have not detected them with an upper limit on the column density of about 10^{12} cm^{-2}, assuming an excitation temperature of 7 K. Similarly to the cold core L1689B studied by Bacmann et al. (2012) we also detect ketene (CH_2CO), with a column density of $\sim 3 \times 10^{12}$ cm^{-2} in complete agreement with the column densities determined for L1689B. In addition to the main isotopologues of the detected species, we also detect transitions of the deuterated counterparts CH_3CCD and CH_2DOH. The deuteration level is estimated to be about 0.045 for CH_3CCH and 0.055 for CH_3OH, however, this deuteration fractions should be better constraint with future observations of other transitions and with higher spectral resolution (necessary to resolve the lines). The uncertainty of the column density listed in Table 2 does not includes the uncertainty in the linewidth, which can not be measured in our coarse spectral resolution observations. The column densities can differ by 30% if the linewidth is increased/decreased by 0.1 km s^{-1}, or by 50% if the variation is 0.2 km s^{-1}. Therefore, the column densities reported in Table 2 have to be considered with caution. High-spectral resolution observations are necessary to improve the determination of the excitation temperature and column density. Another source of uncertainty in the column density determination is the excitation temperature: Observations of more transitions for the different molecules are required to better constraint the column density and to search for non-LTE effects.

In general, a number of deuterated compounds have been detected: DCS^+, HDCS, NH_2D, c-C_3HD, c-C_3D_2, CH_2DOH and CH_3CCD. The deuteration fraction is 0.2 for H_2CS, 0.07 for c-C_2HD, and about 0.05 for CH_3CCH and CH_3OH. It is worth noting that the column density measured for c-C_3HD and c-C_3D_2 is in agreement with the recent measurements of Spezzano et al. (2013).

Finally, in addition to the COMs discussed above, we highlight the detection of some species: (*a*) HCS^+ has been observed in previous surveys towards Taurus molecular cores (e.g. Ohishi & Kaifu 1998; Kaifu et al. 2004). Here, we present for the first time, a tentative detection of the deuterated counterpart DCS^+. A detailed study of different deuterated species may help to better understand the routes of deuteration, in particular for those more complex species, and to compare with similar studies conducted in high-mass star forming regions (e.g. Fontani et al. 2011, 2015); (*b*) Similarly, we report for the first time a tentative detection of $HOCO^+$ in this source, for which we determine a column density of $\sim 2 \times 10^{11}$ cm^{-2}; and (*c*) The detection of HCO is common in photon-dominated regions (PDRs; e.g. Schilke et al. 2001), where the chemistry is dominated by the presence of large amounts of far-UV photons. The Taurus molecular cloud is a low-mass star forming complex, and therefore there are no high-mass stars in the region able to produce enough UV photons. In this survey we report the detection of HCO in a cold, dense core, not associated with a PDR, with a column density of $\sim 10^{12}$ cm^{-2}. Bacmann & Faure (2016) studied HCO in a number of cold prestellar cores, and related its abundance with that of other species such as H_2CO, CH_3O and finally CH_3OH. The authors determine the abundance ratios between the different species to be HCO:H_2CO:CH_3O:CH_3OH $\sim 10 : 100 : 1 : 100$, when the formation of methanol occurs via hydrogenation of CO on cold grain surfaces. The observed abundances of the intermediate species HCO and CH_3O suggest they are gas-phase products of the precursors H_2CO and CH_3OH, respectively. We measure an abundance ratio of HCO:CH_3OH $\sim 1 : 10$ for our cold, dense core (see Table 2), consistent with the results reported by Bacmann & Faure (2016).

5. Summary

We have used the IRAM 30m telescope to conduct sensitive observations of a cold, dense core in TMC-1C, with the goal of detecting the CO-H_2 van der Waals complex. We have not detected any transition of the CO-paraH_2 and CO-orthoH_2 compounds with a rms noise level of $\sim$ 2 mK for a spectral resolution of 0.7 km s^{-1}. This sets a new strong upper limit for the abundance of the complex: [CO-H_2]/[CO] $\sim 5 \times 10^{-6}$. We estimate that the expected abundance of the complex, with respect to CO, in the ISM can be $\sim 10^{-8}$–10^{-3}, which suggest that more sensitive observations would be required to search for and detect for the first time the CO-H_2 complex in the ISM.

Our sensitive spectral line survey have revealed the detection of 75 different spectral lines coming from 41 different species (including isotopologues). The excitation temperature is $\sim$ 7 K, consistent with previous estimates. We detect a number of complex organic molecules such as CH_3CN, CH_3OH, CH_3CCH and deuterated isotopologues. The detection of these species in a cold object is consistent with the similar findings in other objects (e.g. L1689B, Bacmann et al. 2012). Future studies of these complex species to better constraint the physical parameters, as well as the study of more rare isotopologues, can help to improve the current understanding of the formation of complex species in the cold ISM.

Acknowledgements. We acknowledge the comments and suggestions of the anonymous referee that helped to improve the manuscript. AP would like to thank Nicolas Billot for his help with the observations and data processing and the IRAM team. This work was supported by Deutsche Forschungsgemeinschaft through grant SFB 956 (subprojects A6, B4 and C3).

References

Allen, R. J., Loinard, L., McKellar, A. R. W., & Lequeux, J. 1997, ApJ, 489, 102
Bacmann, A. & Faure, A. 2016, A&A, 587, A130
Bacmann, A., Taquet, V., Faure, A., Kahane, C., & Ceccarelli, C. 2012, A&A, 541, L12
Blake, G. A., Sutton, E. C., Masson, C. R., & Phillips, T. G. 1987, ApJ, 315, 621
Caselli, P., Walmsley, C. M., Tafalla, M., Dore, L., & Myers, P. C. 1999, ApJ, 523, L165
Cazaux, S., Tielens, A. G. G. M., Ceccarelli, C., et al. 2003, ApJ, 593, L51
Cummins, S. E., Linke, R. A., & Thaddeus, P. 1986, ApJS, 60, 819
Fontani, F., Busquet, G., Palau, A., et al. 2015, A&A, 575, A87
Fontani, F., Palau, A., Caselli, P., et al. 2011, A&A, 529, L7
Garrod, R. T. & Herbst, E. 2006, A&A, 457, 927
Herbst, E. & van Dishoeck, E. F. 2009, ARA&A, 47, 427
Jankowski, P., Surin, L. A., Potapov, A., et al. 2013, J. Chem. Phys., 138, 084307
Kaifu, N., Ohishi, M., Kawaguchi, K., et al. 2004, PASJ, 56, 69
Klemperer, W. & Vaida, V. 2006, Proceedings of the National Academy of Science, 103, 10584
McKellar, A. R. W. 1988, ApJ, 326, L75
Möller, T., Bernst, I., Panoglou, D., et al. 2013, A&A, 549, A21
Möller, T., Endres, C., & Schilke, P. 2015, ArXiv 1508.04114
Müller, H. S. P., Schlöder, F., Stutzki, J., & Winnewisser, G. 2005, Journal of Molecular Structure, 742, 215

Ohishi, M. & Kaifu, N. 1998, Faraday Discussions, 109, 205
Olano, C. A., Walmsley, C. M., & Wilson, T. L. 1988, A&A, 196, 194
Pak, I., Surin, L. A., Dumesh, B. S., et al. 1999, Chemical Physics Letters, 304, 145
Pickett, H. M., Poynter, R. L., Cohen, E. A., et al. 1998, J. Quant. Spec. Radiat. Transf., 60, 883
Potapov, A., Surin, L., & Schlemmer, S. 2015, Journal of Molecular Spectroscopy, 307, 18
Potapov, A. V., Panfilov, V. A., Dolgov, A. A., Surin, L. A., & Dumesh, B. S. 2009a, Optics and Spectroscopy, 106, 655
Potapov, A. V., Surin, L. A., Panfilov, V. A., et al. 2009b, ApJ, 703, 2108
Roberts, H. & Millar, T. J. 2000, A&A, 364, 780
Sánchez-Monge, Á., Beltrán, M. T., Cesaroni, R., et al. 2014, A&A, 569, A11
Sánchez-Monge, Á., Cesaroni, R., Beltrán, M. T., et al. 2013, A&A, 552, L10
Sánchez-Monge, Á., Palau, A., Estalella, R., et al. 2010, ApJ, 721, L107
Schilke, P., Pineau des Forêts, G., Walmsley, C. M., & Martín-Pintado, J. 2001, A&A, 372, 291
Schnee, S., Caselli, P., Goodman, A., et al. 2007, ApJ, 671, 1839
Schnee, S. & Goodman, A. 2005, ApJ, 624, 254
Spezzano, S., Brünken, S., Schilke, P., et al. 2013, ApJ, 769, L19
Spezzano, S., Gupta, H., Brünken, S., et al. 2016, A&A, 586, A110
Surin, L. A., Fourzikov, D. N., Giesen, T. F., et al. 2007, Journal of Physical Chemistry A, 111, 12238
Suzuki, H., Yamamoto, S., Ohishi, M., et al. 1992, ApJ, 392, 551
van Dishoeck, E. F. 2014, Faraday Discussions, 168, 9
Vanden Bout, P. A., Steed, J. M., Bernstein, L. S., & Klemperer, W. 1979, ApJ, 234, 503
Vastel, C., Ceccarelli, C., Lefloch, B., & Bachiller, R. 2014, ApJ, 795, L2

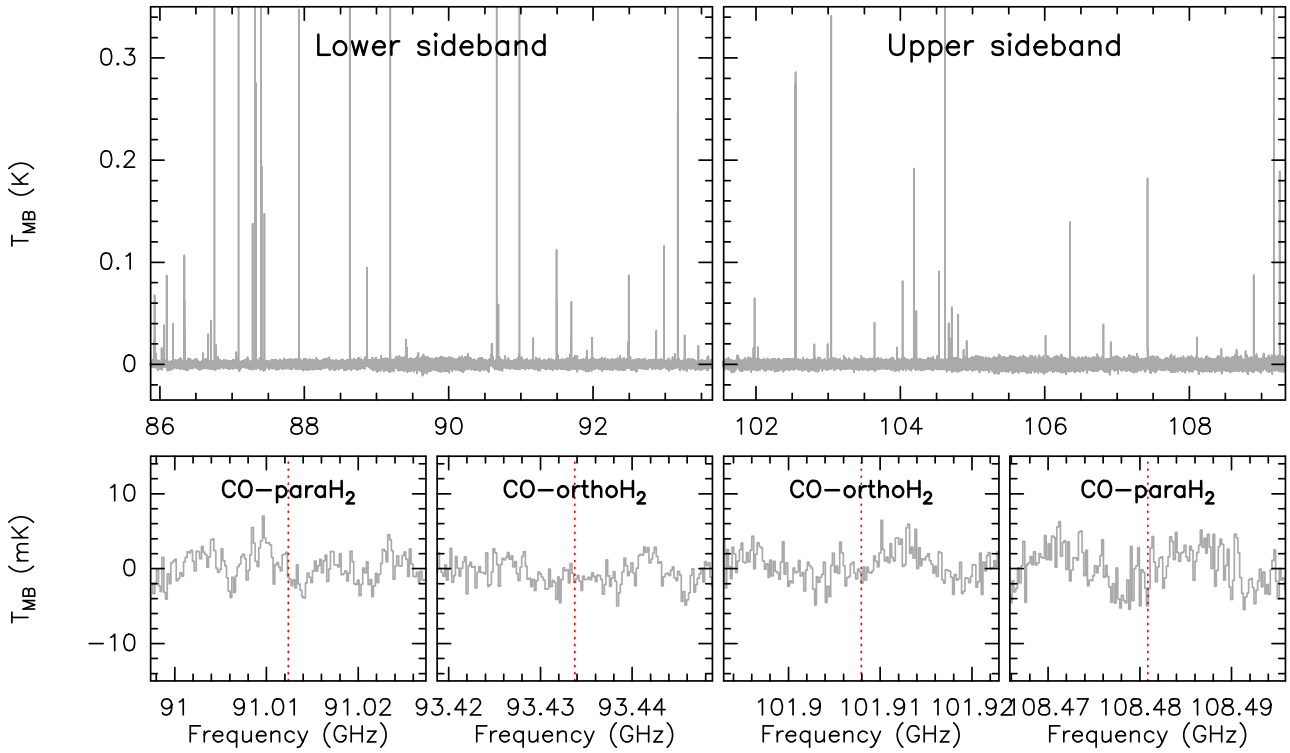

Fig. 2: *Top panels*: Full spectrum observed with the IRAM 30m telescope towards the cold dense core in TMC-1C. The mean rms noise level is $\sim$ 2 mK. Most of the detected lines emit only in one channel (channel width 0.5–0.7 km s^{-1}), suggesting that the linewidth of the different lines is $\leq$ 0.7 km s^{-1} (see Sect. 3.2). *Bottom panels*: Close-up views of the frequency ranges around the brightest transitions of the CO-H_2 van der Waals complex. The corresponding frequencies are listed in Table 1, and are shown in the panels with a vertical dotted line. The expected linewidth is $\approx$ 0.3 km s^{-1}, as measured in higher spectral resolution observations (e.g. Spezzano et al. 2013).

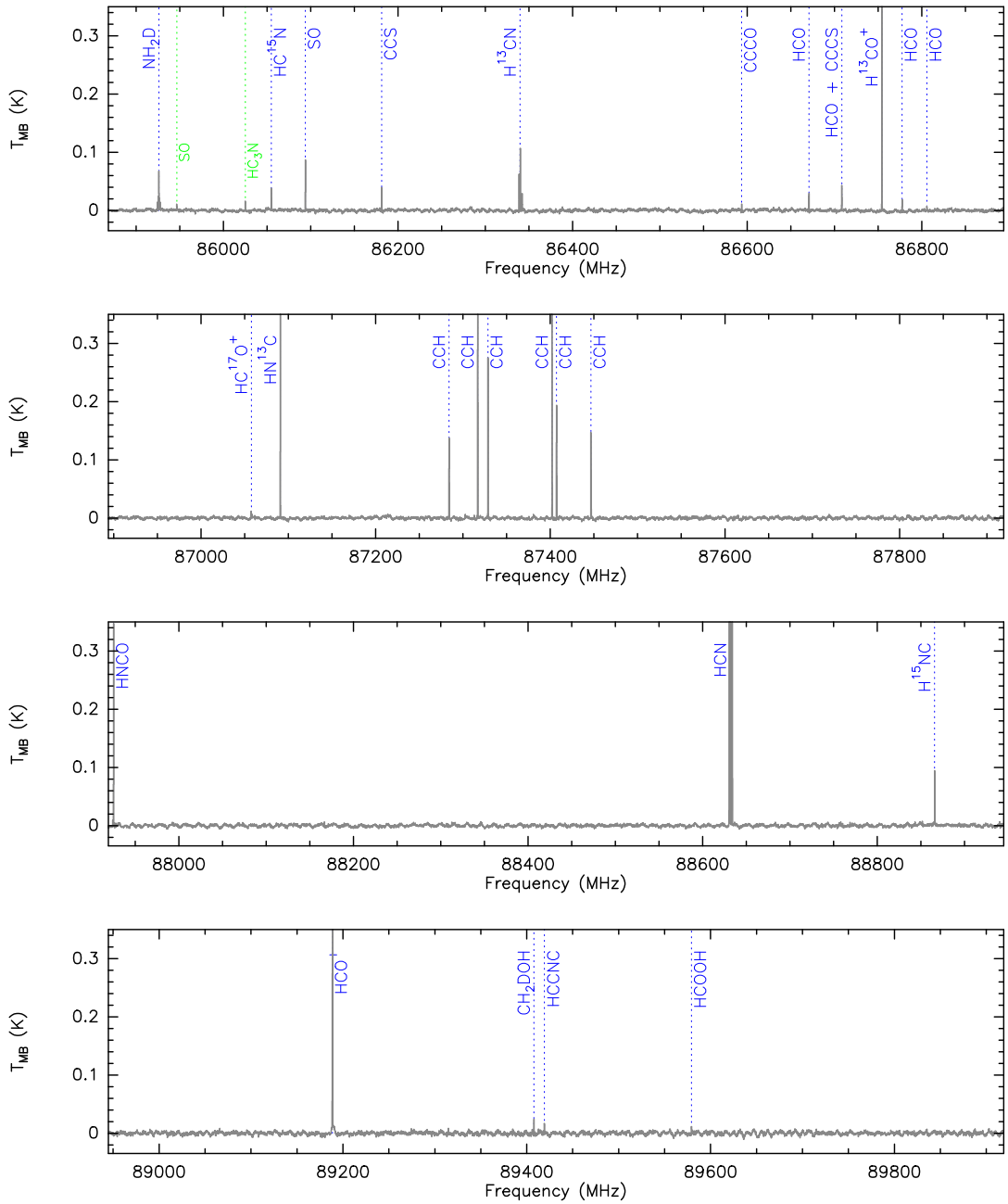

Fig. 3: Spectral line survey towards TMC-1C. Each panel shows about 1 GHz of the total 16 GHz frequency band. The observed spectrum is shown in dark grey. Each identified transition is indicated with a blue dotted line and the name of the corresponding species. The green dotted lines correspond to ghost lines from the image sideband.

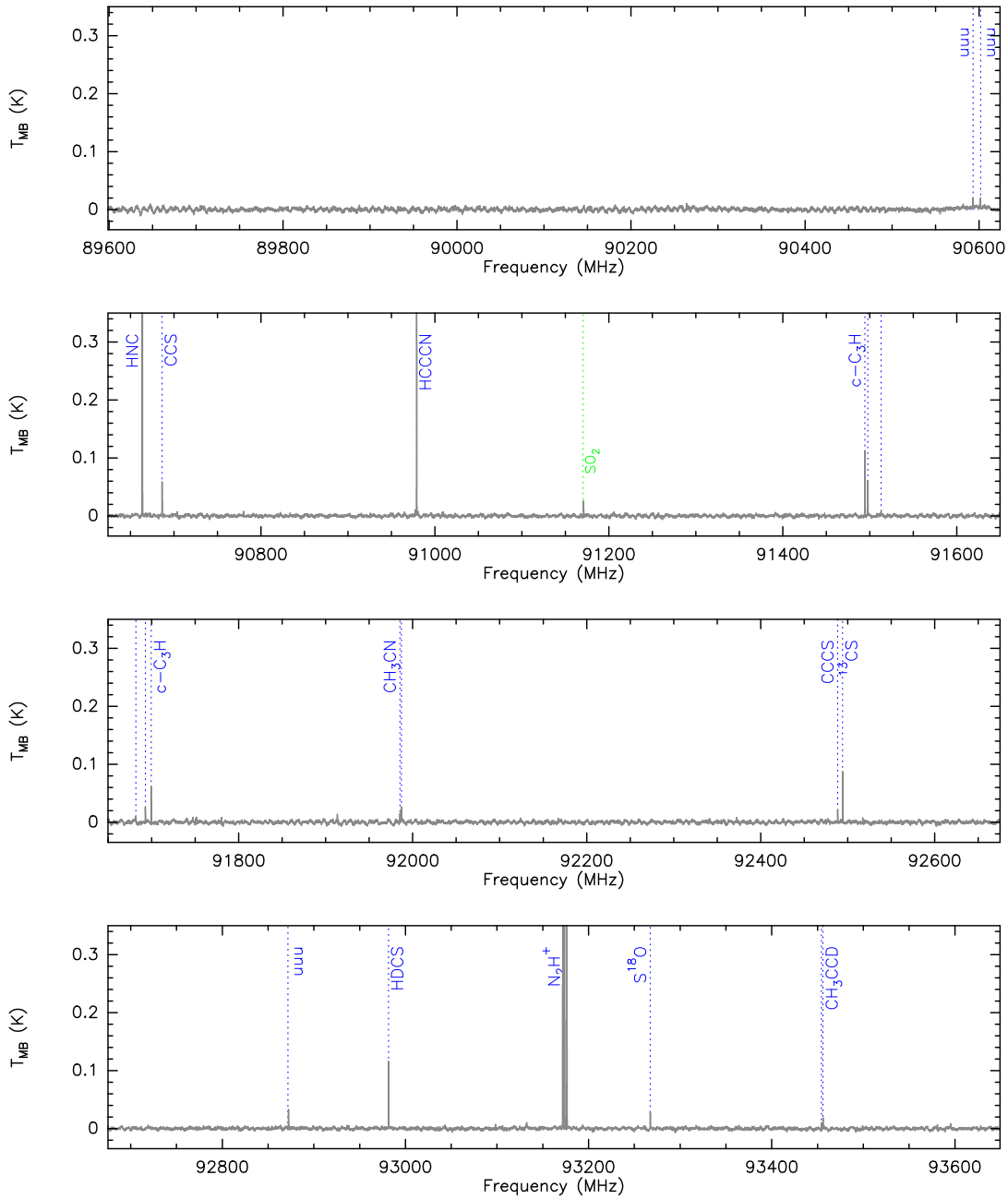

Fig. 3: Continued.

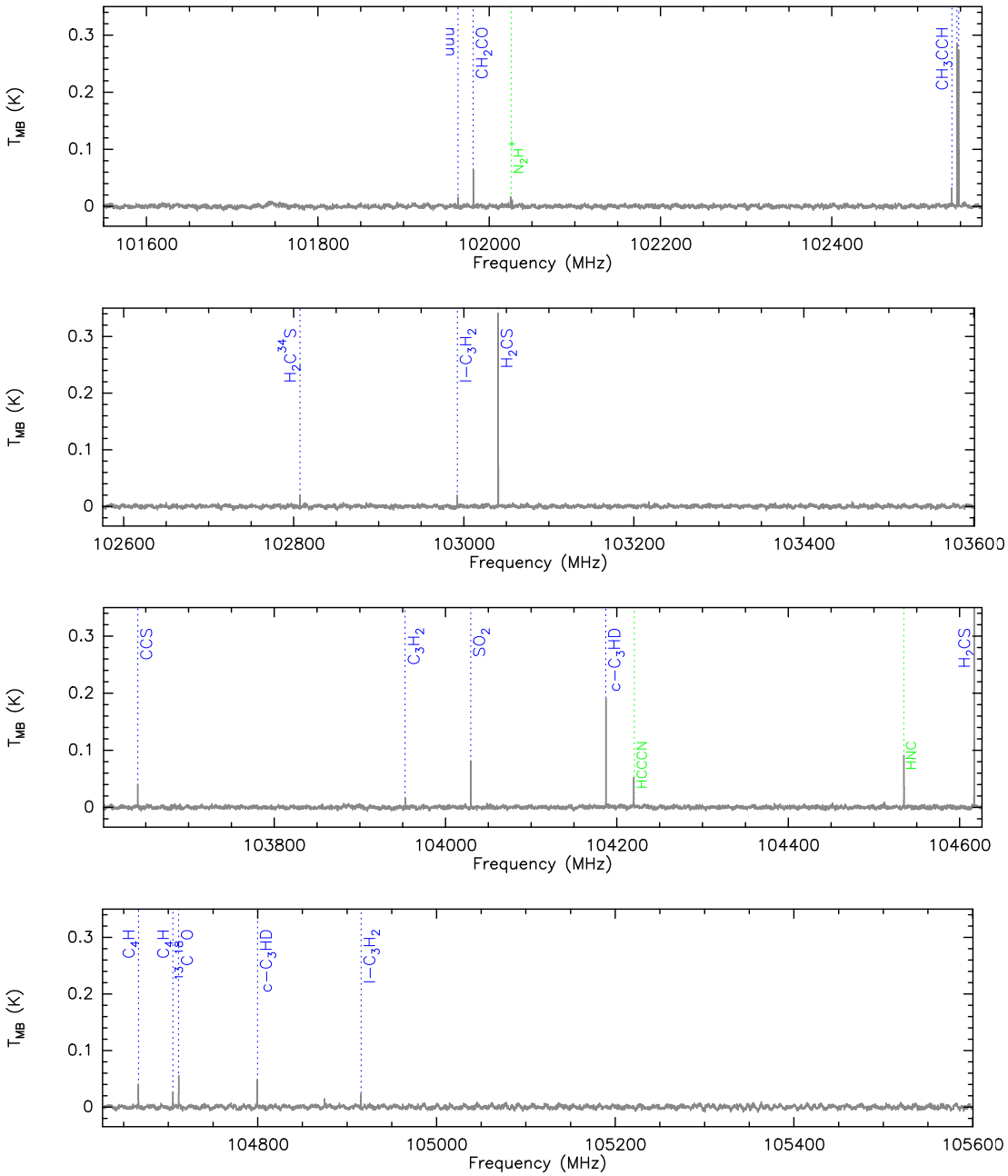

Fig. 3: Continued.

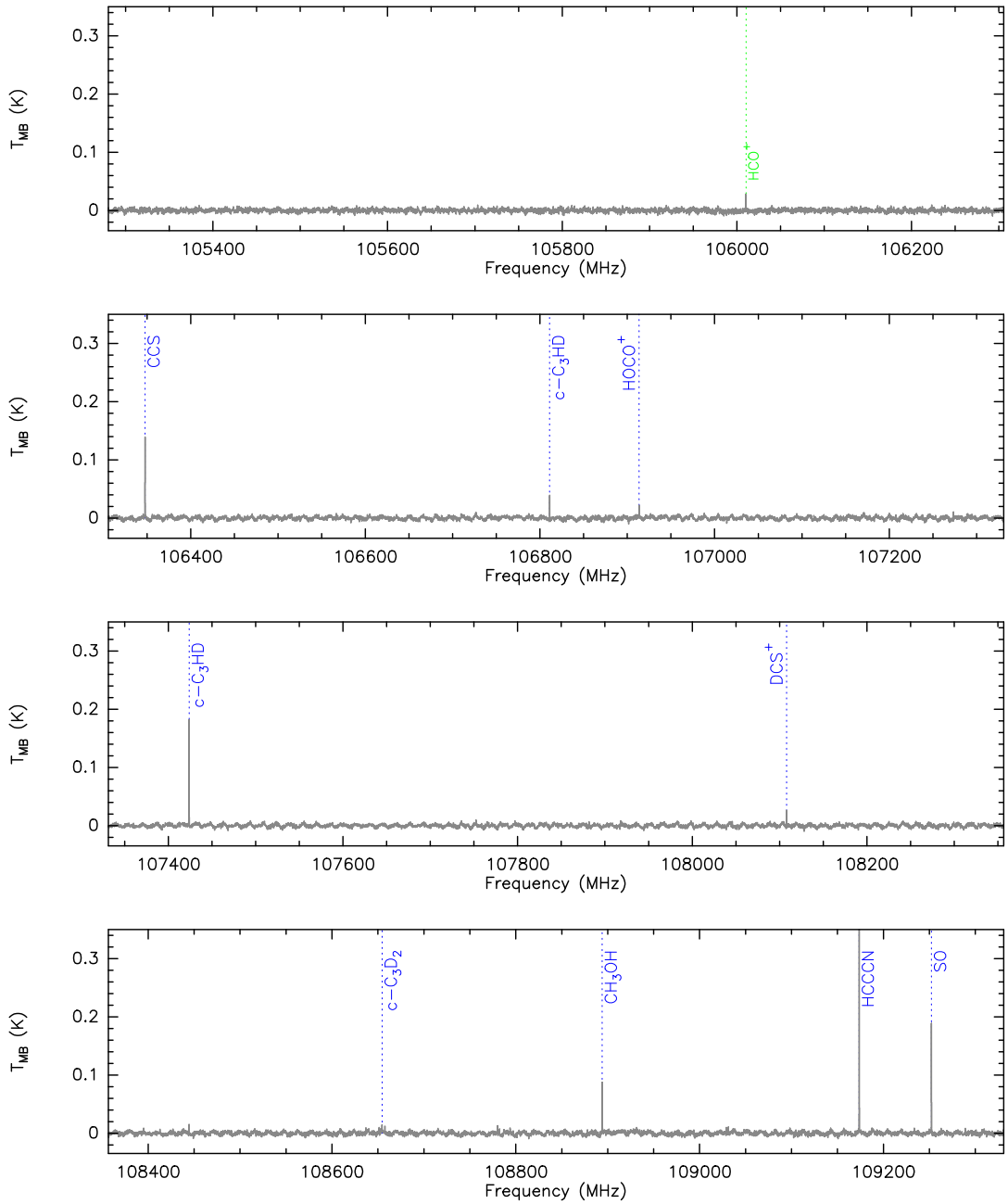

Fig. 3: Continued.